



Relationship Between Coronary Fractional Flow Reserve and Computational Fluid Dynamics Analysis in Moderate Stenosis of the Coronary Artery

Daisuke Kittaka; Hisaya Sato, PhD; Yuichi Nakai, PhD; Kyoichi Kato, PhD

Background: Fractional flow reserve (FFR) is used to evaluate the need for percutaneous coronary intervention (PCI) in cases of moderate stenosis of the coronary artery. Recently, diagnostic imaging support with computational fluid dynamics (CFD) analysis has been garnering attention. This study defines the relationship between FFR conducted for cardiac catheterization and CFD analyses conducted using coronary computed tomography (CT) for moderate stenosis, in addition to considering whether wall pressure (WP) and wall shear stress (WSS) can be used to evaluate ischemia.

Methods and Results: Cases in which FFR was measured via coronary CT and cardiac catheterization was performed within 3 months were collected retrospectively. In the CFD analysis, WP and WSS were calculated and compared with FFR. Three groups were created to compare results of CFD analysis and FFR values according to the location of the stenosis: the right coronary artery, the left anterior descending artery, and the left circumflex artery. There was a correlation between FFR and WSS according to CFD analysis for moderate stenosis of the coronary artery, with a cut-off value for treatment able to be calculated.

Conclusions: The results of this study suggest that ischemia can be evaluated by conducting CFD analysis (WSS) using coronary CT.

Key Words: Computational fluid dynamics (CFD); Fractional flow reserve (FFR); Focal stenosis lesion; Wall shear stress (WSS)

Fractional flow reserve (FFR) is conducted to evaluate the need for percutaneous coronary intervention (PCI) for moderate stenosis of the coronary artery. FFR is calculated by measuring the pressure within the coronary artery proximal and distal to the coronary artery stenotic lesion. For example, an FFR of 0.50 means that the actual blood flow is only 50% of the maximum blood flow you would normally see because of the stenosis. Normally, PCI is used when FFR is >0.80 .¹⁻³

Computational Fluid Dynamics (CFD) is the study of understanding the mechanism of the “flow” created when the fluid represented by air and water moves, taking a physical and engineering approach.⁴⁻⁶ CFD is a simulation method used to compute approximate solutions by discretizing the Navier-Stokes equation, an equation that describes the movement of viscous fluids and is used to understand hemodynamics. The advantages of using CFD are that large-scale research facilities are not needed and there is no cost associated with repeating analyses multiple times. Conversely, a disadvantage of CFD is that errors may be introduced as a result of the various hypotheses and models used in the equation. Because of the evolution in

computational ability, CFD analyses can now be performed using general-purpose computers and CFD software.

Recently, blood flow simulations have been adopted in the medical field.⁷ In the congenital heart disease field, because morphology is anatomically complex and there are dynamic changes in blood flow after surgery, CFD has been used to predict hemodynamics since 1995, contributing to the determination of surgical indications and understanding postoperative hemodynamics.^{8,9} Moreover, most vascular diseases, such as thrombosis, arteriosclerosis, and formation of aneurysms, of the human circulatory system occur at junctions and in curved sections of relatively large vessels, as well as in the lower reaches of constricted parts. Clinical studies and autopsies have demonstrated that formation of aneurysms appear locally at sites where the blood flow is disturbed in a hydrodynamic view, suggesting that there is a relationship between blood flow and the onset of vascular diseases.¹⁰ Many studies have also been conducted in the cerebrovascular field using CFD, including the prediction of which aneurysm will rupture among unruptured cerebral aneurysms found occasionally,¹¹ analysis of the flow within the aortic arch, which has various

Received July 21, 2020; accepted July 21, 2020; J-STAGE Advance Publication released online September 25, 2020

Department of Radiological Technology, Showa University Hospital, Tokyo (D.K., H.S.); Showa University Graduate School of Health Sciences, Tokyo (H.S., K.K.); Department of Radiological Technology, Showa University Northern Yokohama Hospital, Yokohama (Y.N.); and Showa University Radiological Technology, Tokyo (K.K.), Japan

Mailing address: Daisuke Kittaka, MS, Department of Radiological Technology, Showa University Hospital, 1-5-8 Hatanodai, Shinagawa-ku, Tokyo 142-8666, Japan. E-mail: d-kittaka@cmed.showa-u.ac.jp

All rights are reserved to the Japanese Circulation Society. For permissions, please e-mail: cr@j-circ.or.jp

ISSN-2434-0790



Table. Patient Characteristics	
Sex (n)	
Male	167
Female	62
Age (years)	72±11
Location of stenotic lesion (n)	
RCA	52
LAD	134
LCx	43
QCA	
% Stenosis	51.7±18.7
MLD (mm)	2.3±0.7
Plaque volume (mm ³)	29.9±11.8
MLA (mm ²)	3.1±0.39
No coronary risk factors	24 (10.5)
Hypertension	163 (71.2)
Diabetes	93 (40.6)
Hyperlipidemia	22 (9.6)
Dyslipidemia	102 (44.5)
Smoking (including past smoker)	70 (30.6)
Hyperuricemia	34 (14.8)
Old myocardial infarction	84 (36.7)
Chronic renal failure	48 (21.0)
Family history of coronary event	29 (12.7)

Unless indicated otherwise, data are given as the mean±SD or as n (%). LAD, left anterior descending artery; LCx, left circumflex artery; RCA, right coronary artery; MLA, minimum lumen area; MLD, minimal lumen diameter; QCA, quantitative coronary angiography.

kinks, and the study of fluid dynamics with regard to the form of arcs and the onset of aneurysms.¹²⁻¹⁶

In the present study, we revealed the relationship between FFR, which is determined during intracardiac catheterization for moderate stenosis of the coronary artery, and CFD analysis using cardiac computed tomography (CT), and then examined whether CFD can be used to evaluate ischemia.

Methods

Materials

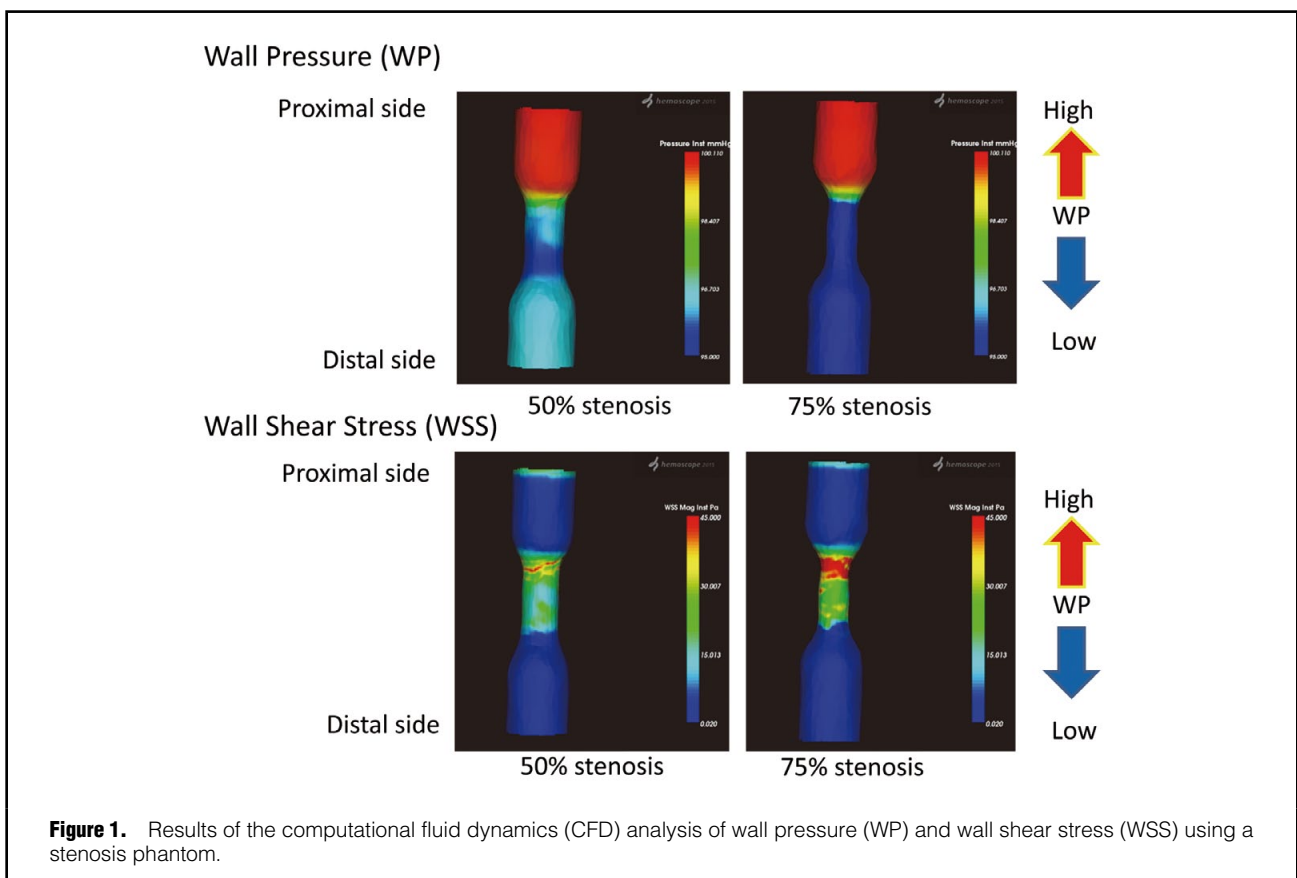
Angiograms were performed using a PHILIPS Allura Xper FD 10/10, CT was performed using a SIEMENS SOMATOM Force CT scanner, 3-dimensional (3D) analysis was performed using an AMIN ZIO Station 2 workstation, and CFD analysis was performed using HemoScope 2015 software. A stenosis phantom was used in the phantom experiment.

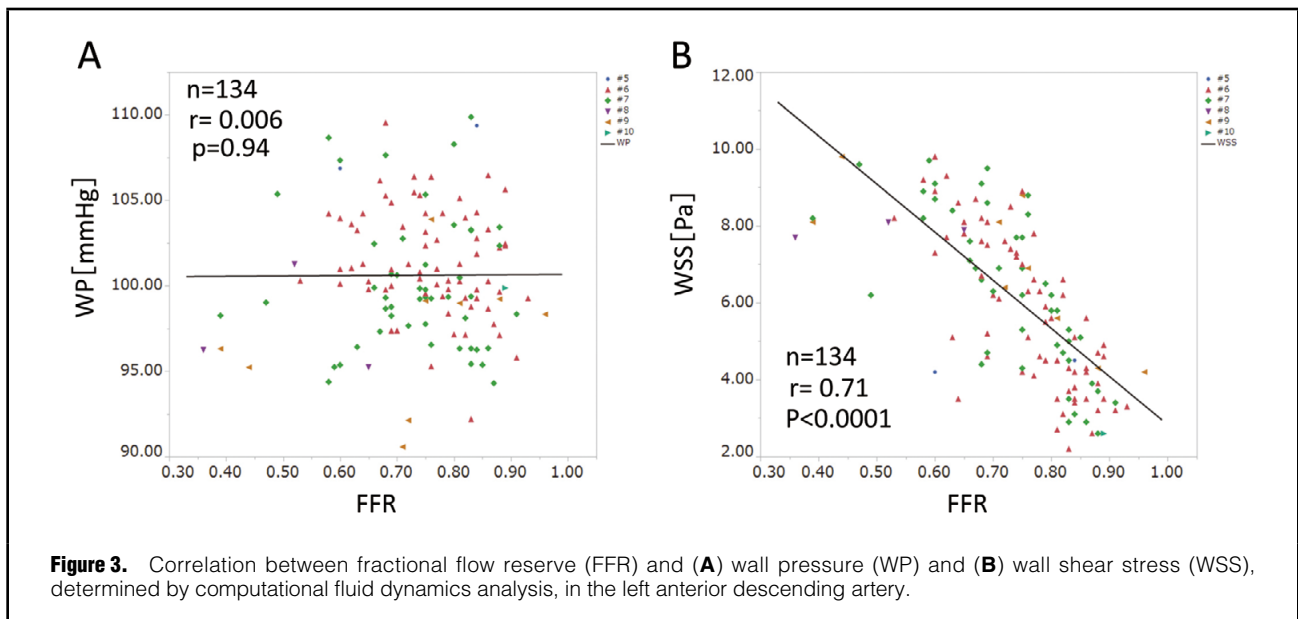
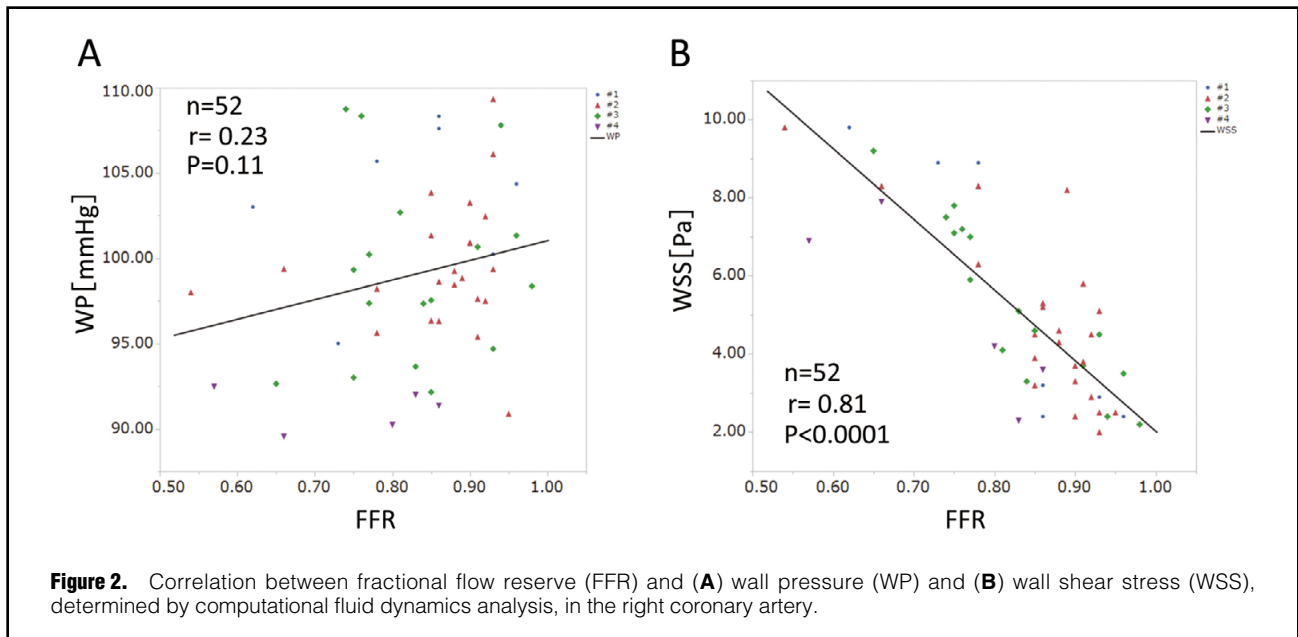
Patients

Information was collected retrospectively for patients with coronary CT-identified moderate stenosis in the coronary arteries and in whom FFR was measured by cardiac catheterization within 3 months between January 2013 and March 2020 (Table).

Basic Examination Using a Stenosis Phantom

CFD analysis was conducted for constricted parts using a stenosis phantom with known stenosis rates. The blood vessel diameter of the stenosis phantom was 5.00 mm and





the stenosis rates were 50% and 75%. Contrast medium was loaded inside the stenosis phantom and images were obtained using CT. The CT images obtained were then used to create volume rendering images. CFD analysis was conducted on the volume rendering images and the behavior of wall pressure (WP) and wall shear stress (WSS) on the stenotic lesion were confirmed. The WP and WSS thresholds were fixed. Blood flow simulation was conducted using a CT image (512×512 pixels, slice thickness 0.75 mm, slice interval 0.6 mm). CFD analysis software hemoscope 2015 was used to extract blood vessels. The half-value method was used to evaluate blood vessels. Blood was defined as an incompressible Newtonian fluid with a density (ρ) of 1,050 kg/m³ and viscosity (μ) of 0.004 Pa·s. A steady

flow was used for the analysis. The finite volume method was used for analysis of the flow equation. A 3D unsteady calculation method was used. The computational mesh of the major area consisted of a tetra mesh with a model length of 0.2 mm. The mesh of the boundary layer area was a prism mesh of the wall-nearest grid (height 0.05 mm, width 0.2 mm). The time acceleration item of the Navier-Stokes equation was calculated using the Euler equation, whereas the space acceleration item was a second-order upwind differencing scheme.

Relationship Between FFR and CFD Analysis

The WP and WSS of CFD analyses calculated using FFR were compared with the results of coronary CT in patients

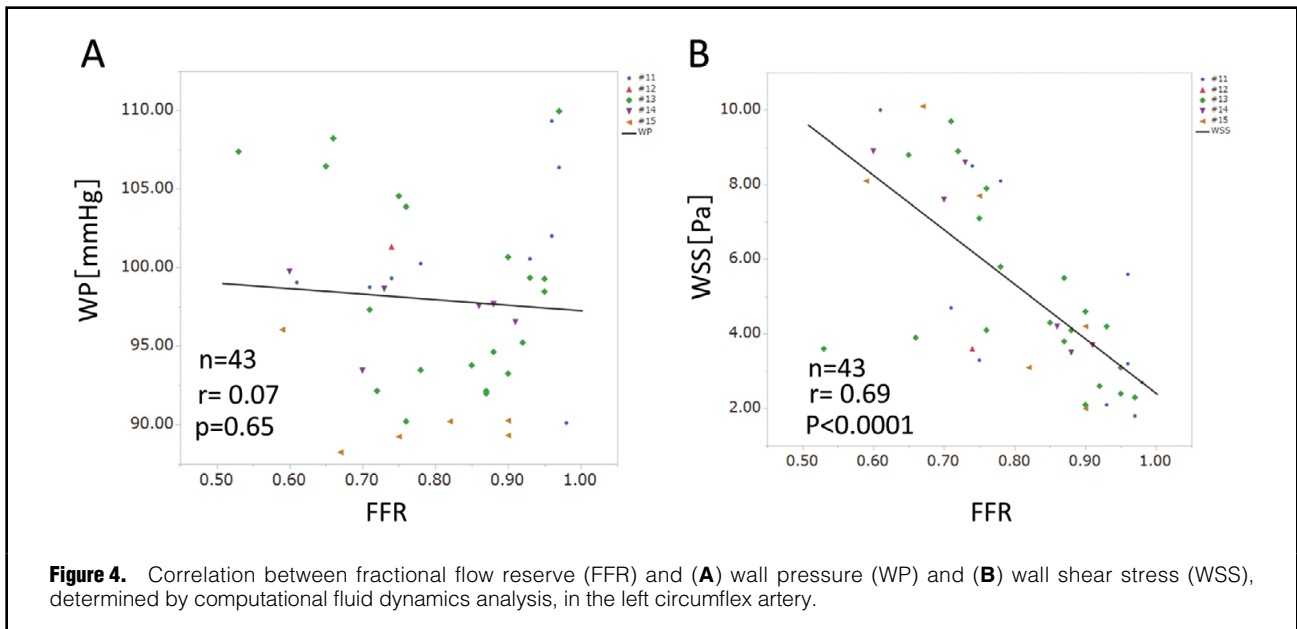


Figure 4. Correlation between fractional flow reserve (FFR) and (A) wall pressure (WP) and (B) wall shear stress (WSS), determined by computational fluid dynamics analysis, in the left circumflex artery.

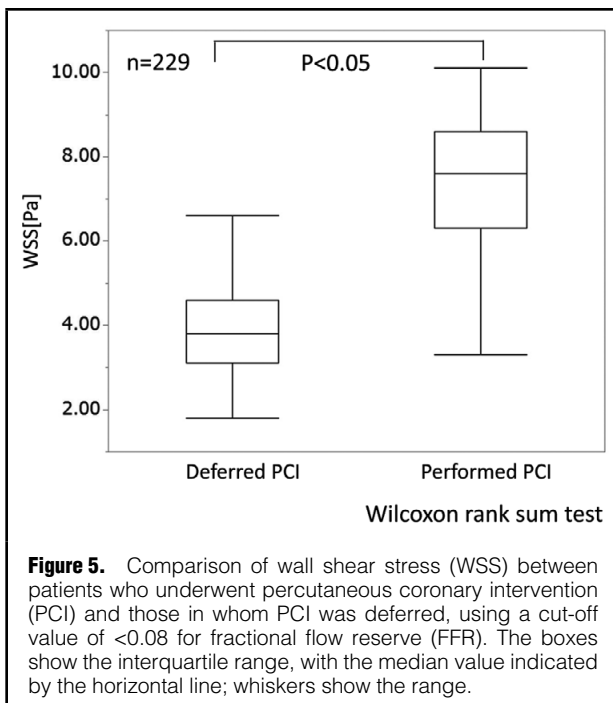


Figure 5. Comparison of wall shear stress (WSS) between patients who underwent percutaneous coronary intervention (PCI) and those in whom PCI was deferred, using a cut-off value of <0.08 for fractional flow reserve (FFR). The boxes show the interquartile range, with the median value indicated by the horizontal line; whiskers show the range.

included in this study. The parameters of CFD analysis were the same as described above. A telediastolic volume rendering image from the coronary CT was used in the CFD analysis. The CT imaging conditions were 120 kV, automatic milliamperes, and pitch 1.5. In the CFD analysis, WP and WSS were calculated and compared with FFR. Three groups were created for comparison of the results of CFD analysis and FFR values depending on the location of the stenotic lesion: the right coronary artery (RCA), the left anterior descending artery (LAD), and the left circumflex artery (LCx). The results of CFD analysis and FFR values were compared in each group.

Receiver Operating Characteristic Analysis of WSS

Cardiac catheterization yielded 120 lesions with $\text{FFR} < 0.08$ deemed positive and 109 lesions with $\text{FFR} \geq 0.80$ deemed negative. Receiver operating characteristic (ROC) analysis was performed on each coronary artery to determine the WSS cut-off value.

Statistical Analysis

The significance of differences in WSS between patients in whom PCI was performed and those in whom it was deferred was determined using a Wilcoxon rank-sum test. ROC analysis was used to define cut-off values by minimizing the expression $(1 - \text{sensitivity})^2 + (1 - \text{specificity})^2$. Statistical analyses were performed using JMP pro 14. Two-sided $P < 0.05$ was considered significant.

Ethical Considerations

This study was approved by the Ethics Committee of Showa University, Japan. The study was conducted in accordance with the ethical principles based on the Declaration of Helsinki and the ethical guidelines for human medical research, and complied with this study implementation plan.

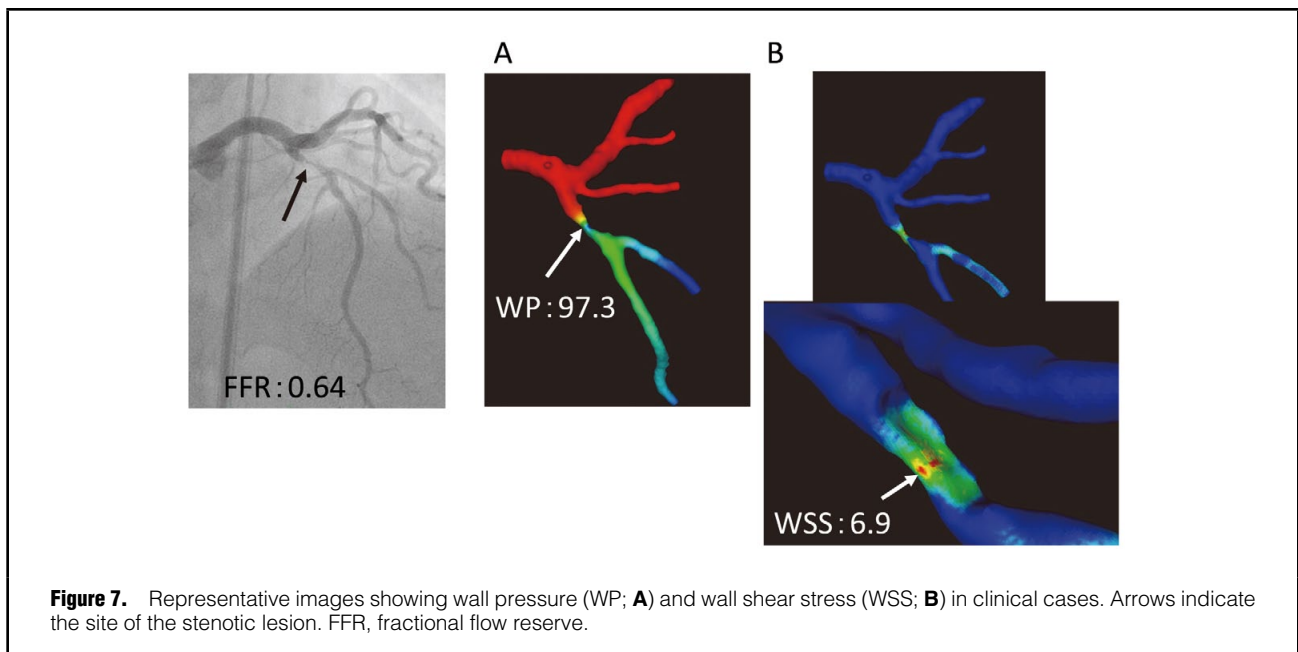
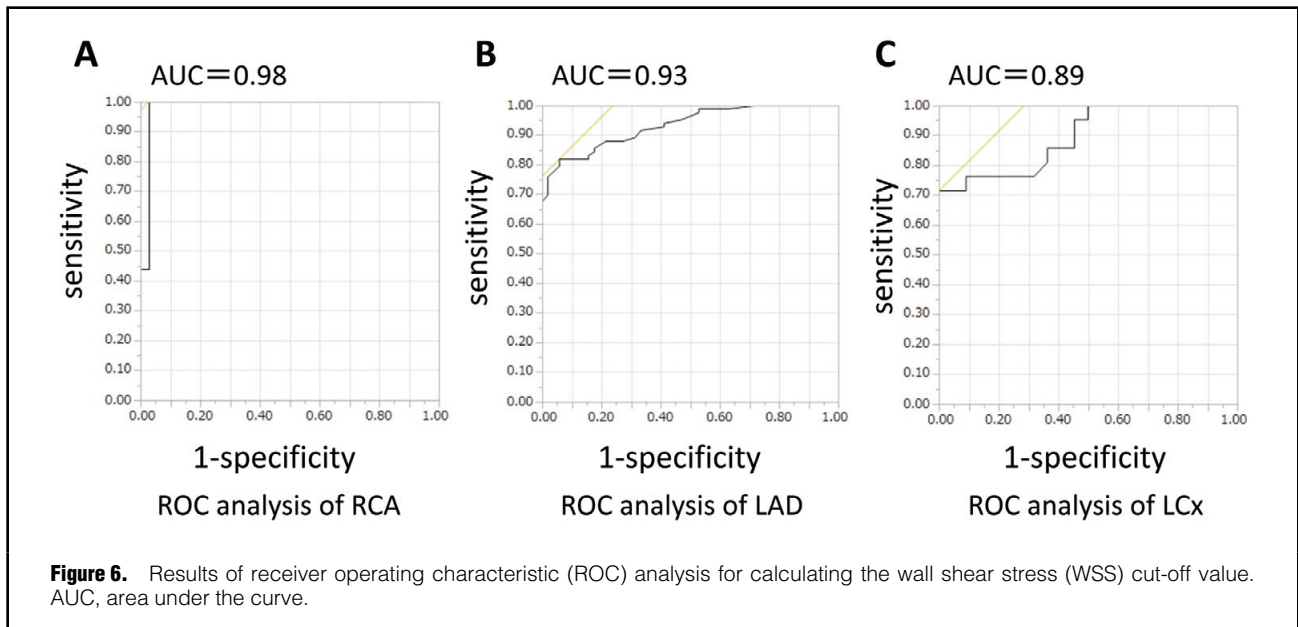
Results

Basic Examination Using a Stenosis Phantom

CFD analysis using a stenosis phantom revealed increasing WP on the proximal side of the constriction site as the stenosis rate of the stenosis phantom increased, and decreasing WP on the distal side. The WSS at the constriction site was also increased with an increasing stenosis rate of the stenosis phantom (Figure 1).

Relationship Between FFR and CFD Analysis

No correlation was seen between WP determined by CFD analysis and FFR for each segment of the RCA in 52 patients with ischemic heart disease, with a correlation coefficient (r) of 0.23 (Figure 2A). There was a tendency for WP to be higher on the proximal side of the lesion as the



degree of stenosis. Conversely, the WSS of CFD analysis in each segment of the RCA was correlated with FFR ($r=0.81$; **Figure 2B**).

Similarly, for each segment of the LAD in 134 patients with ischemic heart disease, there was no correlation between WP determined by CFD analysis and FFR ($r=0.006$; **Figure 3A**). There was a tendency for WP to be higher on the proximal side as the rate of stenosis increased, similar to findings in the RCA. Conversely, there was a correlation for WSS determined by CFD analysis in each segment of the LAD and FFR ($r=0.71$; **Figure 3B**).

WP determined by CFD analysis in each segment of the LCx in 43 patients with ischemic heart disease was not correlated with FFR ($r=0.07$; **Figure 4A**). Conversely, there

was a correlation between WSS determined by CFD analysis in each segment of the LCx and FFR ($r=0.69$; **Figure 4B**). Setting a cut-off value for FFR of 0.80, WSS was significantly higher in the group of patients in whom PCI was performed than in those in whom the procedure was deferred (**Figure 5**).

ROC Analysis of WSS

Using ROC analysis of cut-off values of WSS at an FFR of <0.80 revealed that the sensitivity and specificity of a WSS cut-off value of 598 kPa (5.9 atm) were 100% and 97.2%, respectively, in the RCA (**Figure 6A**) and 81.9% and 94.1%, respectively, in the LAD (**Figure 6B**). At a cut-off value of 588 kPa (5.8 atm) for WSS in the LCx, sensitivity

and specificity were 71.4% and 100%, respectively (Figure 6C).

Discussion

Basic Examination Using a Stenosis Phantom

In the basic examination using a stenosis phantom, WP was high on the proximal side of the stenosis phantom and low on the distal side. Based on Bernoulli's law, because fluid flow velocity is faster at constricted parts than in parts with no stenosis, the WP at the site of constriction decreased when fluid flowed through the constricted part. The stenosis phantom used for the basic examination in this study demonstrated that WP was low after passing through the constricted part. The cause of this is considered to be energy loss due to the detachment of flow after constriction. Conversely, WSS at the constricted part increased as the stenosis rate of the stenosis phantom increased. It was assumed that the values of WSS was high because of the emergence of a vortex at the constricted part.

Relationship Between FFR and CFD Analysis

CFD analysis using clinical cases with focal stenosis showed that WP increased on the proximal side of the stenosis (Figure 7A). The greater the degree of stenosis, the greater the pressure loss after the stenosis. Therefore, if WP after the stenosis is low, it is considered that ischemia is present distal to the stenosis. However, WP was not correlated with FFR in each coronary artery. This is probably because the degree of pressure loss varies depending on the location of the stenosis.

Conversely, in clinical cases, WSS increased in the stenosis, which was considered to be due to turbulent flow in the stenosis, as in the basic examination in the stenosis phantom (Figure 7B). WSS was correlated with FFR because the WSS at the stenosis increases as the stenosis increases. Moreover, using a cut-off value of 0.80 for FFR revealed that WSS was significantly higher in patients who underwent PCI than in those in whom PCI was deferred. This can be explained by sections with both high and low forces rubbing against the vascular wall because of biologic factors, pathologic stenosis, junctions, etc. in the blood vessels, in addition to the occurrence of a vortex and turbulent flow at the site of constriction.

Reynolds number (Re) is used to determine whether flow is likely to be laminar or turbulent. The Re of coronary flow is $800 < \text{Re} < 1,000$. Generally, Re is used as an indicator to indicate the transition from laminar to turbulent flow, with flow becoming turbulent when Re is $> 2,300$.¹⁷ The velocity of fluid flow is faster when the stenosis is larger. We believe that because Re increases if viscosity is low and the velocity of fluid flow is fast, as is the case for blood, turbulent flow occurs easily. When flow transitions to turbulent flow, stress is likely to appear in vessels, with increases in both mean WSS experienced by the vascular wall and variation components in the blood, because mixing inside the fluid is facilitated.

ROC Analysis of WSS

Using cut-off values of WSS of 598 kPa (5.9 atm) in the RCA and LAD and 588 kPa (5.8 atm) in the LCx at an FFR of < 0.08 , resulted in sensitivity and specificity of 100% and 97.2%, respectively, in the RCA, 81.9% and 94.1%, respectively, in the LAD, and 71.4% and 100%, respectively, in the LCx. Using the stenosis phantom, the

cut-off value of WSS when the stenosis rate was 75%, which is considered a significant stenosis in coronary arteries, was 608 kPa (6.0 atm). The cut-off values for WSS calculated by ROC analysis in clinical cases were 598 kPa (5.9 atm) for the RCA and LAD and 588 kPa (5.8 atm) for the LCx, which are equivalent to the value determined in the phantom experiment. Therefore, the WSS cut-off value for each coronary is considered to have high validity. Thus, evaluating ischemia by calculating the WSS using CFD analysis for moderate stenosis of the coronary artery is considered possible.

We believe that a comparison of the diagnostic accuracy following evaluation of FFR in CT angiography is necessary. Driessen et al reported a diagnostic accuracy, sensitivity, and specificity of 87%, 90%, and 86%, respectively, for FFRCT < 0.80 identifying stenosis $> 90\%$.¹⁸ Conversely, Nakazato et al reported a diagnostic accuracy, sensitivity, and specificity of 71%, 74%, and 67%, respectively, for lesions of intermediate stenosis severity.¹⁹ CFD analysis using FFR with a WSS cut-off value < 0.80 has a high per-vessel sensitivity and specificity, and can be considered a useful technique.

The present study has some limitations. First, CFD analysis is significantly affected by the images used in the analysis. It is unclear to what degree blood vessel diameter and CT value of the 3D construction image affected the results of the CFD analysis in this study.

Conclusions

We revealed the relationship between FFR, which is calculated during intracardiac catheter testing for moderate stenosis of the coronary artery, and CFD analysis using cardiac CT images. The findings suggest that evaluating ischemia of coronary arteries is possible by calculating the WSS using CFD analysis of cardiac CT images.

Sources of Funding

This study did not receive any specific funding.

Disclosures

There is no conflict of interest to disclose.

IRB Information

This study was approved by the Ethics Committee of Showa University, Japan (Reference no. 2783).

References

1. Bech GJ, De Bruyne B, Pijls NH, de Muinck ED, Hoorntje JC, Escaned J, et al. Fractional flow reserve to determine the appropriateness of angioplasty in moderate coronary stenosis: A randomized trial. *Circulation* 2001; **103**: 2928–2934.
2. Pijls NHJ, van Schaardenburgh P, Manoharan G, Boersma E, Bech JW, van't Veer M, et al. Percutaneous coronary intervention of functional nonsignificant stenosis: 5 year follow up of the DEFER study. *Am J Coll Cardiol* 2007; **49**: 2105–2111.
3. De Bruyne B, Fearon WF, Pijls NHJ, Barbato E, Tonino P, Piroth Z, et al. Fractional flow reserve-guided PCI for stable coronary artery disease. *N Engl J Med* 2014; **371**: 1208–1217.
4. Libby P, Okamoto Y, Rocha VZ, Folco E. Inflammation in atherosclerosis: Transition from theory to practice. *Circ J* 2010; **74**: 213–220.
5. Chatzizisis YS, Jonas M, Coskun AU, Beigel R, Stone BV, Maynard C, et al. Prediction of the localization of high-risk coronary atherosclerotic plaques on the basis of low endothelial shear stress: An intravascular ultrasound and histopathology natural history study. *Circulation* 2008; **117**: 993–1002.
6. Hwang J, Saha A, Boo YC, Sorescu GP, McNally JS, Holland

- SM, et al. Oscillatory shear stress stimulates endothelial production of O₂ from p47phox-dependent NAD(P)H oxidases, leading to monocyte adhesion. *J Biol Chem* 2003; **278**: 47291–47298.
7. Takao H, Yamamoto M, Otsuka S, Suzuki T, Masuda S, Murayama Y, et al. Analysis of cerebral aneurysms using computational fluid dynamics (CFD). *Jpn J Neurosurg* 2012; **21**: 298–305.
 8. Itatani K, Miyaji K, Tomoyasu T, Nakahata Y, Ohara K, Takamoto S, et al. Optimal conduit size of the extracardiac Fontan operation based on energy loss and flow stagnation. *Ann Thorac Surg* 2009; **88**: 565–573.
 9. Itatani K, Miyaji K, Nakahata Y, Ohara K, Takamoto S, Ishii M. The lower limit of the pulmonary artery index for the extracardiac Fontan circulation. *J Thorac Cardiovasc Surg* 2011; **142**: 127–135.
 10. Wada S, Nokari T, Naiki T. Effects of physical and hydrodynamic factors on the localization of vascular disease. *Electronic Sci Res* 1997; **4**: 22–32.
 11. Yagi T, Qian Y, Takao H, Murayama Y, Umezu M. Toward establishing medical engineering technology to predict rupture of cerebral aneurysm. *Artif Organs* 2010; **39**: 227–231.
 12. Mori D, Yamaguchi T. Computational hydrodynamic analysis of the effect of intra-aortic blood flow in the development of aortic aneurysm. *J Jpn Coll Angiol* 2003; **43**: 94–97.
 13. Fung YC. *Biomechanics: circulation*. New York: Springer Verlag, 1997; 58–69.
 14. White FM. *Viscous fluid flow*. McGraw-Hill, 2005; 1259–1269.
 15. Takao H, Murayama Y, Otsuka S, Qian Y, Mohamed A, Masuda S, et al. Hemodynamic differences between unruptured and ruptured intracranial aneurysms during observation. *Stroke* 2012; **43**: 1436–1439.
 16. Miura Y, Ishida F, Umeda Y, Tanemura H, Suzuki H, Matsushima S, et al. Low wall shear stress is independently associated with the rupture status of middle cerebral artery aneurysms. *Stroke* 2013; **44**: 519–521.
 17. Takagi S, Matsumoto Y. Multiphase flows in bio-medical field. *Jpn J Multiphase Flow* 2012; **26**: 386–391.
 18. Driessen RD, Danad I, Stuijzand WJ, Rajmakers PG, Schumacher SP, van Diemen PA, et al. Comparison of coronary computed tomography angiography, fractional flow reserve, and perfusion imaging for ischemia diagnosis. *J Am Coll Cardiol* 2019; **73**: 162–173.
 19. Nakazato R, Park HB, Berman DS, Gransar H, Koo BK, Erglis A, et al. Noninvasive fractional flow reserve derived from computed tomography angiography for coronary lesions of intermediate stenosis severity: Results from the DeFACTO Study. *Circ Cardiovasc Imaging* 2013; **6**: 881–889.